Room-Temperature Surface Modification of Cu Nanowires and Their Applications in Transparent Electrodes, SERS-Based Sensors, and Organic Solar Cells

Xiao Wang,[†,‡] Ranran Wang,*,[†] Haitao Zhai,[†,‡] Xi Shen,[§] Tao Wang,[†,‡] Liangjing Shi,[†] Richeng Yu,*,[§] and Jing Sun*,[†]

[†]State Key Laboratory of High Performance Ceramics and Superfine Microstructure, Shanghai Institute of Ceramics, Chinese Academy of Sciences, Shanghai 200050, China

[‡]University of Chinese Academy of Sciences, Beijing 100049, China

[§]Beijing National Laboratory for Condensed Matter Physics, Institute of Physics, Chinese Academy of Sciences, Beijing 100190, China

Ⓢ Supporting Information

ABSTRACT: Cu nanowires (Copper nanowires) have attracted lots of attention recently due to their potential applications in transparent electrodes, surface enhanced Raman scattering (SERS) based sensors, and solar cells. However, as the surface composition and morphology of Cu nanowires severely influence the performance of the devices based on them, facile surface modification methods need to be developed. Herein, we propose a room-temperature, time-saving aqueous solution method, through which clean Cu nanowires with small Ag nanoparticles decorating around them could be achieved. The unique "sesame candy bar" structure of Cu nanowires brought about significant enhancement on the electrical, optical, and mechanical performances of Cu nanowire networks. Transparent electrodes with ideal opto-electrical performance (47 Ω sq^{-1} @ 89.1% T) and high antioxidation, antithermal, and electrical stability were fabricated. Stretchable electrodes based on the modified Cu nanowire networks showed superior stretch-ability and cyclic stability. SERS sensors and organic solar cells based on Cu nanowire networks exhibited high performance due to the enhanced surface plasmonic coupling and light scattering effect. We believe that the method will shed light on the large-scale fabrication and application of Cu nanowire based devices.

KEYWORDS: copper nanowires, surface modification, copper nanowire electrodes, surface-enhanced Raman, organic solar cells
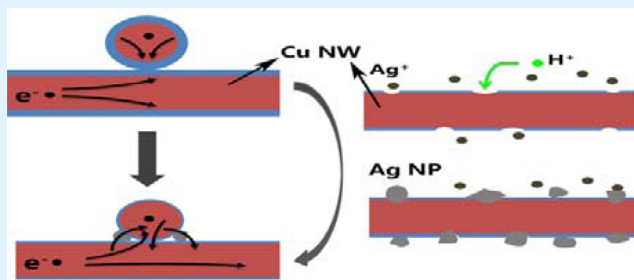
1. INTRODUCTION

Metal nanowires have attracted lots of attention in recent years for their potential applications in transparent electrodes,[1−3] flexible electronics,[4−6] SERS-based sensors,[7−9] solar cells,[10,11] and catalysts for water oxidation.[12] Among the most commonly used metal nanowires, silver nanowires are widely concerned due to their high conductivity, stability, flexibility, and superior plasmonic effects. By modifying their surface, high performance transparent electrodes, organic solar cells with power conversion efficiency of 7.99% (1.09 times the power conversion efficiency of the solar cells based on ITO),[10] and SERS-based sensors with improved sensitivity[8] have been fabricated. Apart from Ag nanowires, Cu nanowires have also attracted lots of attention during recent years for their high conductivity, sufficient flexibility, and low cost. Researchers fabricated high performance transparent electrodes, flexible electrodes as well as solar cells[2,13−15] based on Cu nanowires synthesized through chemical methods.

The morphology and component on the surface of metal nanowires have a great influence on the electrical, optical, and mechanical properties of their assemblies.[7,16−18] Organic molecules such as capping agents or dispersants often reside on the surface of metal nanowires after synthesis, which will severely hinder the intertransportation of electrons between adjacent nanowires and increase the junction resistance. Besides, oxide layers are also ubiquitous on the surface of metal nanomaterials considering their high activity, which further increases the junction resistances. Therefore, the removal of these unfavorable surface impurities is the precondition of obtaining high performance metal nanowire based electrical devices. The optical properties of metal nanowires can also be tuned by surface optimization. Researchers have found that Ag nanowires with nanoparticles

decorated around their surface exhibit a superior SERS enhancement factor[7] and improved light scattering effects.[8]

In order to get high performance devices based on metal nanowires, surface modification methods have been developed to optimize the surface of the nanowires. Annealing is the most commonly used one in removing the impurities and forming welded electron paths.[3,14,19] However, an annealing process usually involves high temperature and protective gas,[14] which is unsuitable for fabricating large-scale and flexible electrodes. Photothermal methods have also been used to remove the impurities and form solder joints selectively at the junctions, which show some success in improving the conductivity of the nanowire networks.[6,20]

Recently, chemical rinsing and electroless plating have been proposed to modify Cu nanowire electrodes. The chemical approaches are usually carried out at room temperature without any special atmospheric control, which makes it an ideal post-treatment method in the fabrication of flexible and stretchable devices. Won[19] reported a lactic acid treatment method, through which Cu NW transparent electrode with excellent optical-electrical performance was obtained. Unfortunately, the acid treatment made Cu NWs more easily oxidized and extra protection layer had to be deposited. In addition to surface cleaning, chemical treatment often leads to the change in the morphology of the metal nanowires through etching or electroless plating, which will significantly influence the optical properties of the nanowires such as light absorption, scattering, and surface plasmon resonance (SPR) etc. By etching Ag nanowires with NH_4OH/H_2O_2 etchant, researchers successfully roughened the surface of Ag nanowires, changed their intrinsic surface plasmon resonance properties and improved their SERS sensing capability.[17] However, as far as we concerned, work still has not been done to adjust the optical properties of Cu nanowires.

Herein, we report a post-treatment method which enables the surface modification of Cu nanowires under room temperature and ambient conditions. The process could be carried out by simply immersing the Cu nanowire films into a solution of $AgNO_3$ and citrate acid (noted as AgCA treatment). Superior to commonly used modification methods like annealing or lactic acid treatment, AgCA method could not only ensure the surface cleaning of Cu nanowires, but also induce the deposition of dense Ag nanoparticles around them, which brought about great enhancement on the electrical, optical and mechanical performance of their assemblies. Transparent electrodes with high opto-electrical performance ($47~\Omega~sq^{-1}$ @ 89.1% T with a figure of merit (FOM) of 67.5) and stability were obtained in less than a minute. Ag nanoparticles deposited around nanowires and at junctions effectively protected the Cu nanowire networks from being damaged by oxidation or mechanical deformation, thus ensuring the fabrication of Cu nanowire electrodes with high stability and ideal flexibility. Apart from high-performance electrodes, due to the enhanced localized SPR effects and improved light scattering effect caused by closely packed silver nanoparticles generated in the treatment process, this unique structure could effectively improve the performance of SERS sensors and organic solar cells based on Cu nanowires. Compared with the devices based on Cu nanowire electrodes post-treated through annealing, improved Raman intensity of Rhodamine 6G (R6G) (an improvement of 4000%) and power conversion efficiency (an improvement of 68%) were detected.

2. RESULTS AND DISCUSSION

In order to get Cu nanowires with uniform diameters and high aspect ratios, we utilized a method similar to the one reported previously by Zhang.[3] Cu nanowires synthesized through this method show an average diameter of 55 nm and a length of 80 μm (Figure S1a of the Supporting Information, SI). Their high aspect ratios make them great candidates for fabricating high performance transparent electrodes. The as-prepared Cu nanowires were then dispersed in toluene and deposited on a cellulose membrane through vacuum filtration to fabricate uniform networks. Nanowire films were transferred to other substrates like glass slide, silicon wafer, and Polyethylene terephthalate (PET) to be further tested. Figure 1a shows a
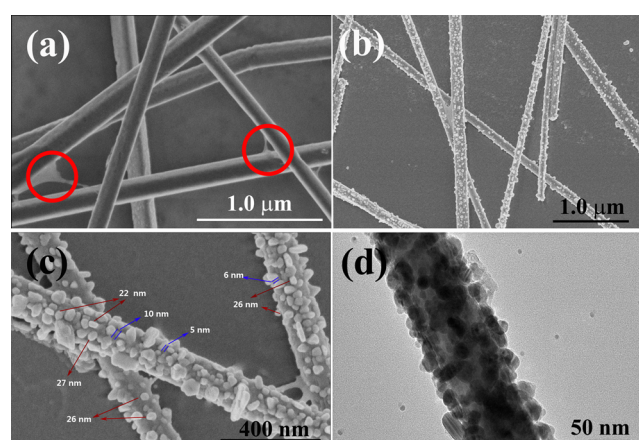

Figure 1. (a). SEM image of the as-prepared Cu nanowire network. (b,c) SEM images of Cu nanowire networks treated by the AgCA method. (d). TEM image of Cu nanowires modified by the AgCA method.

scanning electron microscopy (SEM) image of the as-prepared Cu nanowire film, organic residues can be clearly seen around the nanowires, which cannot be effectively removed only by the common rinsing process. Besides, an oxide layer around the Cu nanowire is inevitable as copper in nanoscale is susceptible to oxidation. X-ray photoelectron spectroscopy (XPS) analysis was performed to give more accurate information on the oxides (Figure S2). The presence of $Cu(OH)_2$ (with a binding energy of 953.1 eV) and CuO (with a binding energy of 933.2 eV) was confirmed through the XPS spectra analysis. After being etched for 10 s by argon ions, the peaks corresponding to $Cu(OH)_2$ and CuO significantly reduce or even disappear, indicating that the oxides mainly present on the surface of the nanowires. Organic residues and oxides around the Cu nanowires block the transportation of electrons between neighboring nanowires and cause high resistance. The as-prepared films usually show high sheet resistance (larger than $10^6~\Omega~sq^{-1}$) and cannot be used as electrodes.

By simply immersing the Cu nanowire networks into a solution of $AgNO_3$ and citric acid, we can effectively modify the surface of the nanowires. Micromorphology characterization and XPS analysis were carried out to understand the mechanism of the surface modification process. Detailed descriptions of these experiments can be found in the Experimental Section.

As shown in the dark field microscopy images of Cu nanowire networks before and after AgCA treatment (Figure S1), no obvious changes in the length of the Cu nanowires

happened during the treatment process, which helped in maintaining the high performance of the electrodes. Figure 1b gives the SEM images of the electrodes after the treating process. Compared with the as-prepared ones, Cu nanowires treated through AgCA method showed a relatively clean surface, indicating the effective removal of organic residues. As shown in the Cu $2p_{3/2}$ XPS profiles presented in Figure S2, the AgCA treatment process also induces a reduction of the peak at 934.8 eV (attributed to $Cu(OH)_2$) and the disappearance of the peak at 933.2 eV (attributed to CuO). The changes of the surface chemical states of Cu nanowires confirm the etching of oxide layers during the post-treatment process. When we further looked into the details of the micromorphology of the electrodes after AgCA treatment, Ag nanoparticles with size around 22−28 nm evenly deposited on the surface of nanowires could be observed (Figure 1c,d). Some of the Ag nanoparticles deposited at the junctions between adjacent nanowires could effectively connect them together (Figure S4). Figure S5 gives high-angle annular dark field (HAADF) and annular bright field (ABF) images of Ag nanoparticles deposited on the surface of a Cu nanowire and the selected area electron diffraction pattern of the Cu nanowire post-treated through AgCA method. The results showed that a certain number of Ag nanoparticles were deposited along the same crystal zone axis of the Cu nanowire. However, the Cu nanowires were too thick for us to get clear high resolution scanning transmission electron microscopy (STEM) images of the interface between Cu nanowires and Ag nanoparticles. In order to get a further understanding of the relative positional relationship between Cu nanowire and Ag nanoparticles, the distribution of the two elements in a Cu nanowire after AgCA treatment was tested. No clear boundary was seen between copper and silver, while blue spots representing Cu were seen at some areas of Ag nanoparticles (Figure S6), indicating the interpenetration between these two elements. On the basis of the phenomena shown above, we speculated that direct contacts happened between Cu nanowire and Ag nanoparticles.

In addition to the micromorphology analysis, controlled experiments were also carried out to understand the mechanism of the AgCA modification process. First, we prepared a citric acid solution (Solution A) of the same pH value as the AgCA treatment solution. After being immersed into Solution A for 20 s, Cu nanowires showed a much cleaner surface compared to the as-prepared ones (Figure S7). Pits can be seen on the surface of the Cu nanowires, which may be caused by the uneven etching caused by hydrogen ions. When we further prolonged the treatment time, the detachment of nanowires happened, and the networks were wrecked. Second, we prepared a solution of $Ag(NO_3)$ (Solution B, the same concentration of Ag^+ as the AgCA treatment solution) and post-treated a Cu nanowire network with it for 20 s. Neither Ag nanoparticles nor a decrease of resistance was observed.

On the basis of the experimental results and analyses shown above, we can elucidate the working principles of the AgCA surface modification process as follows. Apart from being the provider of hydrogen ions similar to lactic acid[18] reported by Won et al., citric acid also works as the reducing agent.[21] Hydrogen ions are quite important in the surface modification process as they can effectively etch the organic residues and oxide layers and make Cu nanowires exposed to Ag^+ at certain areas. The reaction between Cu and Ag^+ occurred in these areas and caused the deposition of Ag nanoparticles. These Ag nanoparticles, as well as bare copper, further accelerate the

reduction of silver ions by citric acid, which induces the disorderly deposition of Ag nanoparticles on the Cu nanowires and at junctions, leading to the formation of nanowires with a unique "sesame candy bar" structure.

As shown by the micromorphology characterization results (Figure 1), the AgCA method could effectively modify the surface of Cu nanowires and thus optimize the electrical properties of Cu nanowire electrodes. To verify these effects, opto-electrical performances and stability of Cu nanowire electrodes based on AgCA method were tested (Figure 2). Cu
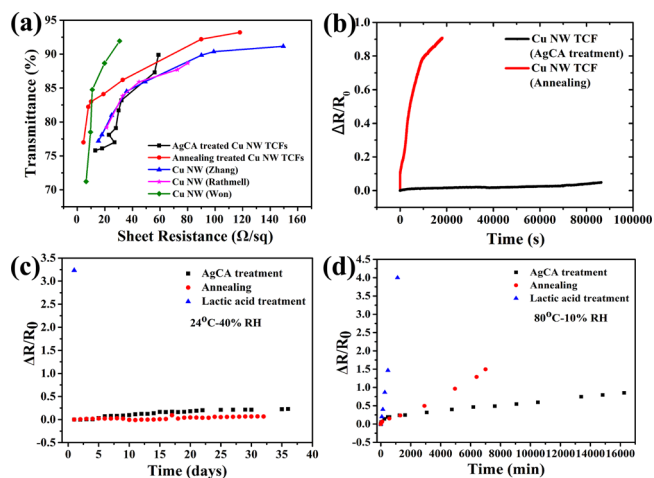
Figure 2. (a) Opto-electrical performances of Cu nanowire films post-treated through different methods. (b) Electrical stability of Cu nanowire electrodes under continuous external bias. (c) Long-term stability of Cu nanowire films post-treated through different methods. (d) Stability of Cu nanowire films post-treated through different methods under harsh environment.

nanowire networks were immersed into the AgCA solution for less than a minute and rinsed with deionized water and ethanol. As shown in Figure S3, the treating effect was greatly influenced by the treatment time and the pH value of the AgCA solution. The best opto-electrical performance was obtained under the treating time of 20 s and pH value of 3.2, which would be applied as the optimum processing parameter in the following work. The figure of merit (FoM)—specific value of DC conductivity (σ_{dc}) and optical conductivity (σ_{op}) is often used to evaluate the opto-electrical performance of metal nanowire networks as applicable electrodes (eq 1).[22,23] A higher FoM represents a lower sheet resistance at higher transmittance, which is preferred in transparent conductive films. The films post-treated by the AgCA method show rival opto-electrical performance (FoM = 67.5) with the films post-treated by annealing (FoM = 74), and even better performances than the Cu nanowire films reported previously (FoM = 53.3[2] and FoM = 47.8[3]).

$$T = \left(1 + \frac{188.5}{R_S}\frac{\sigma_{op}}{\sigma_{dc}}\right)^{-2}$$

(1)

The high conductivity of Cu nanowire electrodes could be attributed to the AgCA surface modification process. Ag nanoparticles deposited at the junctions played a dominant role in connecting adjacent nanowires and forming conductive paths in the networks. In addition, the etching of organic residues and oxides also provided a relatively clean surface and significantly lowered the interface resistance between nanowires (Scheme

1). This outstanding opto-electrical performance indicates the potential of fabricating high-performance large-scale devices

Scheme 1. Illumination of the Working Principles of AgCA Post-Treatment Method
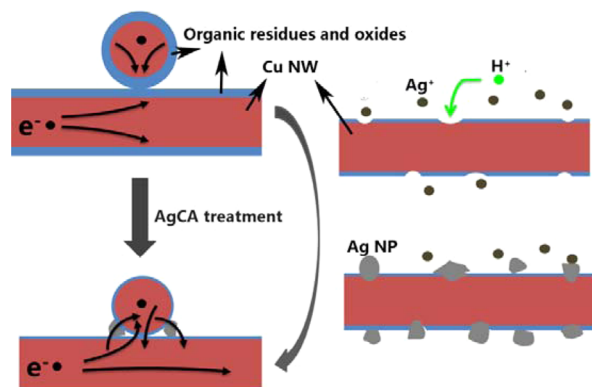
based on Cu nanowire electrodes by the facile, time-saving AgCA method.

According to Figure 1c, silver nanoparticles mainly present around the surface of Cu nanowires, their presence reduces the optical transmittance of Cu nanowire electrodes, and can explain why the opto-electrical performances of our electrodes are slightly worse than the ones post-treated by annealing. However, the existence of silver nanoparticles helps in the improvement of other performances of Cu nanowire electrodes like antioxidation property and electrical stability, which are also quite important for the integrated properties of transparent electrodes.

Herein, the electrical stabilities of the Cu nanowire films post-treated through the AgCA method, lactic acid treatment, and annealing, respectively, were compared. A constant voltage bias of 5 V was applied between two silver paste contacts at opposite ends of the samples. As shown in Figure 2b, the resistance of Cu nanowire transparent electrodes (TEs) post-treated through annealing doubles in less than 300 min. This poor electrical stability is similar to that of the electrodes based on silver nanowires reported previously by Lu et al.[24] and could be explained by the intensively focused Joule heat. On the contrary, as the deposition of silver nanoparticles is not sensitive to the morphology of Cu nanowires, more conductive paths with higher uniformity and lower resistance are created during the treating process, which enables better heat dissipation and effectively avoids the damages caused by focused Joule heating. Cu nanowire electrodes post-treated through AgCA method remained stable even after undergoing a continuous operation of 24 h. This outstanding electrical stability will contribute to the fabrication of more stable devices based on Cu nanowire electrodes. The electrodes post-treated by lactic acid failed soon after the voltage was applied, and we were not able to get valid data. The quick failure of Cu nanowire electrodes might be ascribed to the poor anti-oxidation stability of Cu nanowires treated by lactic acid. High antioxidation stability is also a critical standard for high-performance transparent electrodes. Figure 2c gives the stability of the Cu nanowire electrodes post-treated through different methods at room temperature and 80 °C. Compared with the films post-treated by lactic acid treatment, the films post-treated by the AgCA method and annealing show a much better long-term stability at room temperature, with $\Delta R/R_0$ lower than 0.2

after aging at room temperature for a month. Beside long-term room temperature stability, antithermal stability is also an important factor in the evaluation of transparent electrodes since heat generation phenomenon exists in most electronic devices. The temperature was increased to 80 °C to test the antithermal performances of the films post-treated through different methods. The stability of the Cu nanowire films treated by AgCA method is much better than the ones treated by annealing and lactic acid treatment. This could be explained by the reason that silver were preferentially deposited at the defective sites and protects these vulnerable places from being oxidized. This long-term stability at high temperature makes Cu nanowire electrodes potential alternatives to ITO in electrical devices. The superior electrical, antioxidation, and antithermal stability of Cu nanowire TEs again indicate the advantages of the AgCA post-treatment method.

In addition to providing internanowire pathways for electrons, Ag "bridges" generated through the AgCA process also influenced the mechanical stability of Cu nanowire electrodes by anchoring adjacent nanowires together. Cu nanowire networks modified through AgCA method were transferred to a prestrained substrate to fabricate high performance flexible electrodes (Figure S8). Due to the anchoring effect of Ag nanoparticles and the high aspect ratio, outstanding flexibility and good conductivity of Cu nanowires,[6] Cu nanowire electrodes with improved mechanical stability were fabricated, which show only negligible resistance change within 150% strain. After that, even with the formation of microcracks, the electrode treated by AgCA method still show improved mechanical stability (R/R_0 = 7.8 at 230% strain) compared to the electrodes based on lactic acid treated Cu nanowire networks (R/R_0 = 39 at 230% strain) (Figure S9). This facile AgCA method facilitates the fabrication of high-performance Cu nanowire electrodes under room temperature and thus provides an easy way of fabricating high stretchable electrodes.

Through increasing the surface roughness of Cu nanowires and forming a "sesame candy bar" like structure, AgCA modification method also influenced the optical properties of Cu nanowires and Cu nanowire electrodes. According to SEM images of the Cu nanowire electrodes post-treated by AgCA method, silver nanoparticles with diameters of around 18 nm deposited around the Cu nanowire in a relative dense way and formed a sesame candy bar structure. Nanogaps between adjacent nanoparticles are mostly around 5 to 10 nm (Figure 1c). As reported previously, nanogaps of this size are usually called "hot spots",[25] which can give rise to highly intense and localized electromagnetic fields when excited by incident light of appropriate polarization. These localized fields can effectively enhance the intensity of Raman signals of the organic molecules inside them. Finite difference time domain (FDTD) simulation was performed to give an intuitive exhibition of the enhanced electromagnetic fields at the hot spots. Ag nanoparticles were modeled as hemispheres with a diameter of 20 nm, and a gap distance of 5 nm according to the microstructure characterization results. Figure 3a gives the calculated electric field intensity around a nanowire under a plane light source of 532 nm (near the maximum excitation wavelength of R6G). A highly intense and localized electric field is predicted to exist at the nanogaps and around Ag nanoparticles and decrease significantly beyond them. According to the simulation results, the largest field enhancement factor is around 4. As the Raman enhancement factor is proportional to the fourth power of the
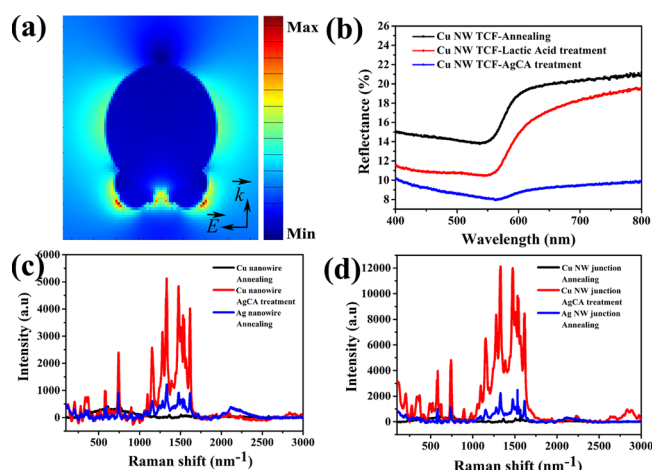
Figure 3. (a) FDTD simulation results of electric density field distribution of the Cu nanowires post-treated through AgCA method at the wavelength of 532 nm and (b) reflectance spectrum of Cu nanowire films post-treated through AgCA method. SERS spectra of rhodamine 6G absorbed onto the surface of (c) a single Cu nanowire and (d) a junction of two adjacent Cu nanowires post-treated through AgCA method.

electromagnetic field enhancement,[26] an upper bond of 256 of the Raman enhancement can be expected. However, as the enhancement mainly happens at the hot spots, the observed factor is lower than 256. The reflectance spectra of the Cu nanowire films with similar thickness (T% ≈ 70%) post-treated by different methods (Figure 3b) were compared to give experimental evidence for the improved light trapping effect. The reflectance of the Cu nanowire films post-treated by lactic acid is slightly lower than the ones post-treated through annealing, which could be attributed to the rougher surface of them. Compared with the Cu nanowire films post-treated by annealing (average reflectance =17.55%) and lactic acid (average reflectance =14.59%), the ones post-treated through our AgCA method show a remarkable broadband reflectance dip (average reflectance =9.07%). The enhanced optical properties (a low reflectance across the whole visible range) of the Cu nanowire films post-treated through AgCA method, which can be attributed to the near-field excitation of localized surface plasmons in silver nanoparticles, are quite favored in SERS-based chemical sensors.[8,27] Apart from the electromagnetic field enhancement effect, surface area and metal species could also influence the SERS enhancement factor.[28] A larger surface area could increase the potential number of molecules that can produce Raman signals while Ag could provide better plasmon resonances properties in the visible/near-infrared range.[28] Compared with smooth Cu nanowires, nanowires with "sesame candy bar" structure have a larger surface area partly covered by silver, which could further enhance the Raman signals.

The Raman signal intensity of R6G using Cu nanowire networks (modified through annealing or AgCA method) and Ag nanowire networks (modified by annealing) as SERS substrates was then detected to test the SERS effect of the electrodes. Spectra were measured at single nanowires and junctions using an excitation source of 532 nm radiation from an Ar+ ion laser (Figure 3). Figures show that the Cu nanowires modified by the AgCA method have the highest SERS enhancement ability both at single nanowires and junctions, the Raman intensity has been improved by a factor of 4000%

(compared to the Cu nanowires modified by annealing) and 250% (compared to the Ag nanowires modified by annealing). We further compared the surface areas and SERS enhancement abilities of different nanowires (see SI) and found that highly localized electromagnetic field generated through strong plasmonic coupling in the sesame candy bar structure is the key reason for achieving ultrahigh sensitivity in SERS-based sensors.[8] This high sensitivity clearly indicates the possible applications of the Cu nanowire films modified through the AgCA treatment method in SERS-based sensors.

In addition to the enhancement of Raman signals, the sesame candy bar structure and the coarse surface of Cu nanowires can also improve the light absorption of the photo active layer in a solar cell through the enhanced light scattering effect.[10] A haze factor measurement was carried out to give evidence on the light scattering and trapping effect. On the basis of the total and diffusive transmittance results of the electrode, we could calculate a haze value of 11.97%, higher than that of the electrodes post-treated through annealing (8.42%) (Figure 4a). The relatively high haze factor confirmed a strong scattering, which is favorable in improving the light absorption of the active layer.[10]
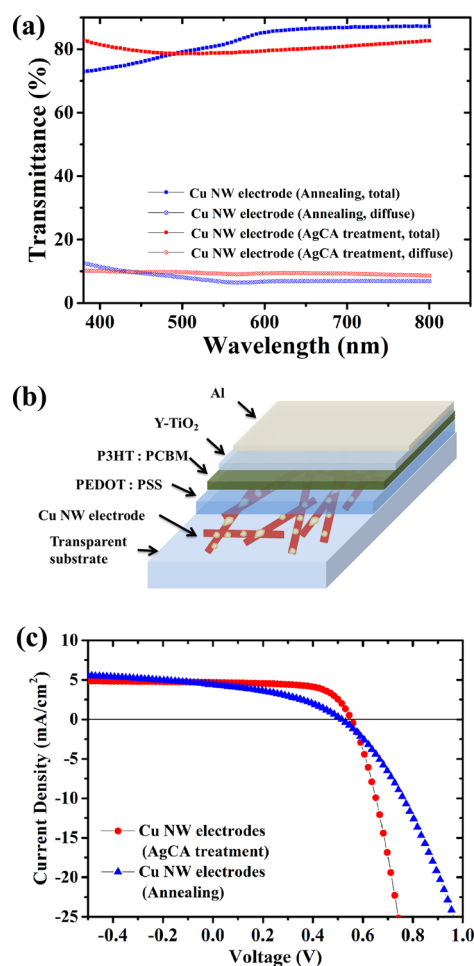

Figure 4. (a) Total and diffuse transmittance of Cu nanowire electrodes post-treated through AgCA method and annealing with total transmittance around 80%. (b). Scheme of the solar cell device based on Cu nanowire electrodes post-treated through AgCA method. (c) J−V curves of solar cells based on Cu nanowire electrodes post-treated through AgCA method and annealing.

By using an in situ polymerization transfer method, we effectively decreased the surface roughness of Cu nanowire electrodes and utilized them in solar cells. Through the fabrication process shown in the Experimental Section, solar cells with a structure shown in Figure 4b were built. The photovoltaic performances of solar cells based on the Cu nanowire electrodes post-treated through annealing and AgCA methods are compared in Figure 4c. While a device based on the Cu nanowire electrode post-treated through annealing shows a power conversion efficiency of 1.25%, with an open circuit voltage (V_{OC}) of 0.514 V, a short circuit current (J_{SC}) of 6.16 mA/cm^2 and a fill factor (FF) of 39.61%, the device based on the Cu nanowire electrode post-treated through AgCA method shows a higher power conversion efficiency of 2.34%, with V_{OC} of 0.553 V, J_{SC} of 6.52 mA/cm^2 and FF of 64.79%. The improved J_{SC} is consistent with the enhanced light scattering effect of the electrode. Ag nanoparticles around the surface of Cu nanowires play an important part in the enhancement of absorption in the photo active layer by not only increasing the optical path length through light scattering, but also improving light trapping by the near-field excitation of localized surface plasmons.[10]

3. CONCLUSIONS

A facile AgCA rinsing method has been developed, which can clean the surface of Cu nanowires and induce the deposition of Ag nanoparticles simultaneously in less than 1 min. The electrical, optical, and mechanical properties of the Cu nanowire networks were significantly optimized through the modification process. Due to the clean surface and Ag nanoparticle bridges generated in the treating process, Cu nanowire networks showed improved opto-electrical performances (FOM = 67.5), higher stability, and enhanced plasmonic coupling and light scattering effect. Moreover, SERS-based sensors with improved SERS enhancement factor (40 times the enhancement factor of the ones treated through annealing) and organic solar cells with enhanced power conversion efficiency were fabricated. We believe this facile, room temperature post-treatment method will open up a new way of utilizing Cu nanowires synthesized through wet-chemical methods in the new born intelligent, flexible electronic, and photovoltaic devices.

4. EXPERIMENTAL SECTION

4.1. Synthesis of Cu Nanowires. Cu nanowires were synthesized through a method similar to the one previously reported by Zhang.[3] Hexadecylamine (HDA) (8 g) and cetyltriamoninum bromide (CTAB) (0.5 g) were mixed and kept at the temperature of 180 °C for about 30 min to form a clear and colorless solution. Copper acetylacetonate was then added to the solution as the copper source. With the help of catalysts, Cu nanowires formed after being kept at a temperature of 180 °C for about 10 h. Typically, preprepared Pt nanoparticles, Ag nanoparticles, or Ni nanoparticles can be used as the catalyst. After the synthesis, Cu nanowires were washed and stored in toluene or ethanol for further research.

4.2. Fabrication of Cu Nanowire Transparent Networks. In order to get high-performance Cu nanowire networks, we filtered Cu nanowires from a homogeneous suspension to a membrane and further transferred them to other substrates such as glass slides, silicon chips, or some polymer substrates. Nitrocellulose membrane (Millipore membrane, 0.22mμm GSWP) was used as the filtration membrane. After the filtration, the membrane with the Cu nanowire film on it was placed on a target substrate and kept at a temperature of 80 °C in a vacuum oven for an hour with a 3 kg weight on it. The

membrane was then removed through an acetone liquid bath, leaving the Cu nanowire networks on the target substrates.

4.3. Post-treatment of Cu Nanowire TEs. A simple, room-temperature post-treatment method was used here to improve the performance of Cu nanowire TEs. The preprepared Cu nanowire networks were immersed into a solution of Ag ions and citric acid at room temperature (AgCA treatment process). The solution was composed of AgNO$_3$ (0.625 mM), citric acid (0.8 mM), and deionized water (200 mL). After the immersing process, Cu nanowire networks were flushed by deionized water and ethanol to remove the residue Ag ions, hydrogen ions, and water. Raman analysis and X-ray photo-electron spectroscopy (XPS) analysis were used to understand the mechanism of the post-treatment methods and test the performances of the electrodes post-treated by this AgCA method. The post-treatment process can also be carried out through simply mixing the dispersion of as-prepared Cu nanowires with the solution of AgNO$_3$ and citric acid.

4.4. Fabrication of Stretchable Electrodes. Cu nanowire electrodes with high stretchability were fabricated on a prestrained, highly stretchable elastomeric eco-flex substrate. The fabrication process was similar to the one reported previously.[5] As-synthesized Cu nanowires were deposited on the filter membrane through vacuum filtration and post-treated through direct immersion into the solution of silver nitrate and citric acid for 20 s. The films with high conductivity were then transferred to half polymerized prestrained Eco-Flex substrates. A higher temperature of 80 °C was needed to complete the polymerization of Eco-Flex and the transfer of Cu nanowire films (Figure S8).

4.5. Fabrication of Organic Solar Cells. Cu nanowire TEs post treated by annealing and AgCA treatment method were transferred to polyacrylate substrates to reduce the surface roughness.[13] PEDOT:PSS bilayer as the hole collecting layers were then formed on the Cu nanowire films by spin coating (3500 rpm for 60 s) and annealing on a hot plate at 130 °C for 30 min in a glovebox. After that, a 100 nm-thick photoactive layer was formed by spin-coating (600 rpm for 60 s) the solution of P3HT: PCBM (20 mg P3HT and 16 mg PCBM in 1 mL orthodichlorobenzene) on the substrate. The photoactive layer was then annealed at 130 °C for 10 min to remove the solution completely. Y-TiO$_2$ was spin-coated (2000 rpm for 60 s) onto the substrate as the electron collecting layer. Finally, the Al top electrode was prepared by thermal evaporation to finish the fabrication process.

4.6. Characterization. The opto-electrical performances of Cu nanowire TEs were tested through a four-point probe (Loresta-EP MCP-T 360) and a UV−vis spectrometer (Lambda 950, PerkinElmer). Raman analysis was performed on a Thermal Scientific DXR laser Raman microspectroscope with a 532 nm excitation length; XPS analysis was carried out on an ESCALAB 250 X-ray photoelectron spectroscope; the tests of electrical stability were performed on a PARSTAT 2273 advanced electrochemical system; The aging tests were carried out at a constant temperature and humidity test chamber (Espec Corp SH-222). Different temperature and humidity conditions of 24 °C −40% (RH) and 65 °C −20% (RH) and 80 °C −20% (RH) were used during the aging tests. For SERS characterization, Cu nanowire films were immersed into ethanol solution containing rhodamine 6G chloride (R6G) (10^{-5} M) as the analyte. Raman measurements were carried out after the evaporation of ethanol. Haze factor was measured on a UV−vis spectrometer (Lambda 950, PerkinElmer). The photocurrent−voltage characterization of organic solar cells was measured with a Keithley 2400 source meter under the simulated AM 1.5G illumination (100 mW/cm^2; Oriel Sol 3A Class AAA Solar Simulator, Newport) calibrated with an optical power meter (Newport, 1918-R).

■ ASSOCIATED CONTENT

ⓢ Supporting Information

The Supporting Information is available free of charge on the ACS Publications website at DOI: 10.1021/acsami.6b08984.

Micromorphology and valence state of Cu nanowires before and after AgCA treatment. Influence of treatment

parameters on the opto-electrical performance of Cu nanowire electrodes. Fabrication and characterization of flexible Cu nanowire electrodes (PDF)

■ AUTHOR INFORMATION

Corresponding Authors
*E-mail: wangranran@mail.sic.ac.cn (R.W.).
*E-mail: rcyu@aphy.iphy.ac.cn (R.Y.).
*E-mail: jingsun@mail.sic.ac.cn (J.S.).

Author Contributions
The manuscript was written through contributions of all authors. All authors have given approval to the final version of the manuscript.

Notes
The authors declare no competing financial interest.

■ ACKNOWLEDGMENTS

■ REFERENCES

(1) Lee, J.; Lee, P.; Lee, H.; Lee, D.; Lee, S. S.; Ko, S. H. Very Long Ag Nanowire Synthesis and its Application in a Highly Transparent, Conductive and Flexible Metal Electrode Touch Panel. *Nanoscale* **2012**, *4* (20), 6408−6414.

(2) Rathmell, A. R.; Wiley, B. J. The Synthesis and Coating of Long, Thin Copper Nanowires to Make Flexible, Transparent Conducting Films on Plastic Substrates. *Adv. Mater.* **2011**, *23* (41), 4798−4803.

(3) Zhang, D.; Wang, R.; Wen, M.; Weng, D.; Cui, X.; Sun, J.; Li, H.; Lu, Y. Synthesis of Ultralong Copper Nanowires for High-performance Transparent Electrodes. *J. Am. Chem. Soc.* **2012**, *134* (35), 14283−14286.

(4) Lee, P.; Ham, J.; Lee, J.; Hong, S.; Han, S.; Suh, Y. D.; Lee, S. E.; Yeo, J.; Lee, S. S.; Lee, D.; Ko, S. H. Highly Stretchable or Transparent Conductor Fabrication by a Hierarchical Multiscale Hybrid Nanocomposite. *Adv. Funct. Mater.* **2014**, *24* (36), 5671−5678.

(5) Lee, P.; Lee, J.; Lee, H.; Yeo, J.; Hong, S.; Nam, K. H.; Lee, D.; Lee, S. S.; Ko, S. H. Highly Stretchable and Highly Conductive Metal Electrode by Very Long Metal Nanowire Percolation Network. *Adv. Mater.* **2012**, *24* (25), 3326−3332.

(6) Han, S.; Hong, S.; Ham, J.; Yeo, J.; Lee, J.; Kang, B.; Lee, P.; Kwon, J.; Lee, S. S.; Yang, M.-Y.; Ko, S. H. Fast Plasmonic Laser Nanowelding for a Cu-Nanowire Percolation Network for Flexible Transparent Conductors and Stretchable Electronics. *Adv. Mater.* **2014**, *26* (33), 5808−5814.

(7) Lee, S. J.; Baik, J. M.; Moskovits, M. Polarization-Dependent Surface-Enhanced Raman Scattering from a Silver-Nanoparticle-Decorated Single Silver Nanowire. *Nano Lett.* **2008**, *8* (10), 3244−3247.

(8) Park, S. G.; Mun, C.; Lee, M.; Jeon, T. Y.; Shim, H. S.; Lee, Y. J.; Kwon, J. D.; Kim, C. S.; Kim, D. H. 3D Hybrid Plasmonic Nanomaterials for Highly Efficient Optical Absorbers and Sensors. *Adv. Mater.* **2015**, *27* (29), 4290−4295.

(9) Formo, E. V.; Mahurin, S. M.; Dai, S. Robust SERS Substrates Generated by Coupling a Bottom-Up Approach and Atomic Layer Deposition. *ACS Appl. Mater. Interfaces* **2010**, *2* (7), 1987−1991.

(10) Wang, B. Y.; Yoo, T. H.; Lim, J. W.; Sang, B. I.; Lim, D. S.; Choi, W. K.; Hwang, D. K.; Oh, Y. J. Enhanced Light Scattering and

Trapping Effect of Ag Nanowire Mesh Electrode for High Efficient Flexible Organic Solar Cell. *Small* **2015**, *11* (16), 1905−1911.

(11) Kim, A.; Won, Y.; Woo, K.; Jeong, S.; Moon, J. All-Solution-Processed Indium-Free Transparent Composite Electrodes Based on Ag Nanowire and Metal Oxide for Thin-Film Solar Cells. *Adv. Funct. Mater.* **2014**, *24* (17), 2462−2471.

(12) Chen, Z.; Rathmell, A. R.; Ye, S.; Wilson, A. R.; Wiley, B. J. Optically Transparent Water Oxidation Catalysts Based on Copper Nanowires. *Angew. Chem., Int. Ed.* **2013**, *52* (51), 13708−13711.

(13) Cheng, Y.; Wang, S.; Wang, R.; Sun, J.; Gao, L. Copper Nanowire Based Transparent Conductive Films with High Stability and Superior Stretchability. *J. Mater. Chem. C* **2014**, *2* (27), 5309−5316.

(14) Ye, S.; Rathmell, A. R.; Stewart, I. E.; Ha, Y. C.; Wilson, A. R.; Chen, Z.; Wiley, B. J. A Rapid Synthesis of High Aspect Ratio Copper Nanowires for High-performance Transparent Conducting Films. *Chem. Commun.* **2014**, *50* (20), 2562−2564.

(15) Zhai, H.; Wang, R.; Wang, W.; Wang, X.; Cheng, Y.; Shi, L.; Liu, Y.; Sun, J. Novel Fabrication of Copper Nanowire/Cuprous Oxide Based Semiconductor-liquid Junction Solar Cells. *Nano Res.* **2015**, *8* (10), 3205−3215.

(16) Goh, M. S.; Lee, Y. H.; Pedireddy, S.; Phang, I. Y.; Tjiu, W. W.; Tan, J. M.; Ling, X. Y. A Chemical Route to Increase Hot Spots on Silver Nanowires for Surface-Enhanced Raman Spectroscopy Application. *Langmuir* **2012**, *28* (40), 14441−9.

(17) Zeng, D.; Chen, Y.; Lu, A.; Li, M.; Guo, H.; Wang, J.; Peng, D.-L. Injection Synthesis of Ni−Cu@Au−Cu Nanowires With Tunable Magnetic and Plasmonic Properties. *Chem. Commun.* **2013**, *49* (98), 11545−11547.

(18) Won, Y.; Kim, A.; Lee, D.; Yang, W.; Woo, K.; Jeong, S.; Moon, J. Annealing-free Fabrication of Highly Oxidation-Resistive Copper Nanowire Composite Conductors for Photovoltaics. *NPG Asia Mater.* **2014**, *6* (6), e10510.1038/am.2014.36

(19) Rathmell, A. R.; Nguyen, M.; Chi, M.; Wiley, B. J. Synthesis of Oxidation-Resistant Cupronickel Nanowires for Transparent Conducting Nanowire Networks. *Nano Lett.* **2012**, *12* (6), 3193−3199.

(20) Garnett, E. C.; Cai, W.; Cha, J. J.; Mahmood, F.; Connor, S. T.; Greyson Christoforo, M.; Cui, Y.; McGehee, M. D.; Brongersma, M. L. Self-limited Plasmonic Welding of Silver Nanowire Junctions. *Nat. Mater.* **2012**, *11* (3), 241−249.

(21) Lu, H.; Zhang, D.; Ren, X.; Liu, J.; Choy, W. C. H. Selective Growth and Integration of Silver Nanoparticles on Silver Nanowires at Room Conditions for Transparent Nano-Network Electrode. *ACS Nano* **2014**, *8* (10), 10980−10987.

(22) Barnes, T. M.; Reese, M. O.; Bergeson, J. D.; Larsen, B. A.; Blackburn, J. L.; Beard, M. C.; Bult, J.; van de Lagemaat, J. Comparing the Fundamental Physics and Device Performance of Transparent, Conductive Nanostructured Networks with Conventional Transparent Conducting Oxides. *Adv. Energy Mater.* **2012**, *2* (3), 353−360.

(23) Hecht, D. S.; Hu, L.; Irvin, G. Emerging Transparent Electrodes Based on Thin Films of Carbon Nanotubes, Graphene, and Metallic Nanostructures. *Adv. Mater.* **2011**, *23* (13), 1482−1513.

(24) Lu, H. F.; Zhang, D.; Cheng, J. Q.; Liu, J.; Mao, J.; Choy, W. C. H. Locally Welded Silver Nano-Network Transparent Electrodes with High Operational Stability by a Simple Alcohol-Based Chemical Approach. *Adv. Funct. Mater.* **2015**, *25* (27), 4211−4218.

(25) Moskovits, M. Surface-enhanced Raman Spectroscopy: a Brief Retrospective. *J. Raman Spectrosc.* **2005**, *36* (6−7), 485−496.

(26) Leem, J.; Wang, M. C.; Kang, P.; Nam, S. Mechanically Self-Assembled, Three-Dimensional Graphene−Gold Hybrid Nanostructures for Advanced Nanoplasmonic Sensors. *Nano Lett.* **2015**, *15* (11), 7684−7690.

(27) Wang, D.; Zhu, W.; Best, M. D.; Camden, J. P.; Crozier, K. B. Wafer-scale Metasurface for Total Power Absorption, Local Field Enhancement and Single Molecule Raman Spectroscopy. *Sci. Rep.* **2013**, *3*, 2867.

(28) Le Ru, E. L.; Etchegoin, P. G. *Principles of Surface Enhanced Raman Speectroscopy*; Elsevier B.V.: Amsterdam, 2008.